Mathematics Letters, 2 (2): 42-56, 2023
eISSN: 2948-3735

COMPUTATIONAL FLUID DYNAMICS STUDY IN MULTI-MICROCHANNELS COOLING SYSTEM

Sharul Azri Bin Noor Azman[1], Nur Farzana Mohd Rasid[2] and Amirah M Sahar[3*]

Pusat Pengajian Sains Matematik, Kolej Pengajian Pengkomputeran, Informatik Dan Matematik, Universiti Teknologi MARA (UiTM), 40450 Shah Alam, Selangor, Malaysia
[1]sharul.azri14@gmail.com, [2]nfarzana79@gmail.com, [3*]amirahsahar@uitm.edu.my
(indicates the corresponding author)*

ABSTRACT

The demand for efficient cooling systems in various industrial applications has prompted the exploration of innovative heat transfer technologies. This research focuses on the computational fluid dynamics (CFD) study of a multi-microchannels cooling system, aiming to enhance thermal management and optimize heat dissipation. The objective of this study is to investigate the flow characteristics, heat transfer performance, and pressure drop behavior within a multi-microchannels cooling system. A numerical simulation approach based on CFD techniques is employed to analyze the fluid flow and heat transfer phenomena. The cooling system consists of an array of microchannels with intricate geometries, enabling enhanced convective heat transfer and increased surface area for improved thermal dissipation. Initially, a comprehensive literature review is conducted to identify existing studies and advancements in microchannel heat transfer. The CFD simulations are then performed to evaluate the fluid flow distributions, temperature distributions, and heat transfer coefficients within the multi-microchannels system under various operating conditions. The results of this study provide valuable insights into the thermal performance of the multi-microchannels cooling system. The impact of parameters such as fluid flow rate is analyzed and discussed. Furthermore, the findings contribute to the understanding of flow distribution and thermal uniformity within the cooling system, enabling optimization of the design and operational parameters. The outcomes of this research offer significant implications for the development of advanced cooling systems in various industries, including electronics cooling, energy systems, and automotive applications. The computational approach employed in this study provides a cost-effective and time-efficient method for analyzing and optimizing the performance of complex cooling systems.

Keywords*: Computational Fluid Dynamics, Cooling System, Heat Transfer, Microchannels, Thermal Management*

Received for review: 05-09-2023; Accepted: 22-10-2023; Published: 06-11-2023

1. Introduction

Due to their high surface-to-volume ratio and compact design, microchannel heat exchangers have several advantages over macroscale ones. The increasing rate of heat transfer caused by the huge surface to volume ratio makes microchannels suitable for compact heat exchangers. Due to their better capacity for heat transfer, microchannel heat sinks are a good cooling method. In addition, a lot of researchers have been drawn to study flow phenomena in microchannels All papers must be written in English. Use 11-point Times New Roman font throughout the paper except for the section headings that should be 11-point Times New Roman bold. The first paragraph following a heading should not be indented. because of the growing usage of micro heat exchangers and their applications, particularly in cooling high-heat-flux equipment like electronic systems. In order to enhance the design and maximize the performance of microchannel heat exchangers, researchers concentrated on comprehending the features of heat transfer and fluid flow at the micro scale level. The parallel microchannels in microchannel heat sinks is for the liquid coolant to flow through. The development of microfabrication methods has made it possible to create microchannels with micrometer-sized diameters. The solid substrate of the heat sink allows for the conduction of heat from the electronic device to the microchannels, where it is removed by liquid moving through the microchannels, Qu et al. (2006) and Pan et al. (2008).

Tuckerman and Pease's (1981) groundbreaking research on the experimental study of heat transfer of water flowing through silicon wafer microchannels under single-phase laminar circumstances marked the beginning of research on single-phase flow and heat transfer in microchannels. They proposed that when the hydraulic diameter of the microchannel decreases, the working fluid's heat transfer coefficient rises. It was possible to attain head flux values of 790 W/cm^2 to keep the chip temperature below 110°C . Many other researchers have been inspired by this study, and microchannel flow has been acknowledged as a highly effective heat removal method. It is stated by Qin et al. (2023) that the flow distribution between the parallel heat transfer tubes is directly determined by the static pressure distributions in the distribution and collection headers. The static pressure distribution is influenced by the static pressure recovery, friction resistance, and local pressure drop. To maintain great flow homogeneity, each heat transfer tube's equal pressure drop is a need. There are two categories of microchannel heat sinks which are single phase and two phase. The presence or absence of liquid boiling within the microchannels determines the category of microchannels. While two-phase flow is mostly influenced by surface tension force, single phase flow in a microchannel relies on a sensible heat rise to achieve cooling. In this study, we will focus more on single phase flow.

Computational fluid dynamics (CFD) are used in applied mathematics, physics, and computer software to visualise how a gas or liquid flows and how it impacts objects as it passes by. In CFD simulations, the Navier-Stokes energy equation provides the basic explanation of energy associated with the flow behaviour. These equations show the relationship between the velocity, pressure, temperature, and density of a moving fluid. The results of velocity, temperature, pressure, and density in single phase flow in multiple microchannels can be obtained by using CFD. Based on the CFD results that will be obtained at the end of this project, it will be use for the further study for two-phase flow in multi-microchannel. Single-phase flow is use first, to maximize the system. The software that will be use in this project is Ansys software. Ansys is a general-purpose modelling tool that is used to solve a wide range of mechanical issues. These mechanical issues include structural analysis, heat transfer and fluid issues. The accuracy and resolution of the CFD simulation results will depend on the grid that is used, which will also have an impact on the calculation time and amount of detail in the result.

The main objectives of this project are to perform the numerical simulation on multi-microchannel by using Ansys Fluent software. Next, to analyze flow distribution inside the multi-microchannels cooling system. Lastly, to analyze the effect of flow rates on flow distribution.

2. Methodology

There are multiple stages in CFD simulation which are shown as in Figure 1. First stage is pre-processing. This stage consists of getting the geometry and mesh ready for simulation. Importing or constructing the CAD model, cleaning up and repairing model geometry, splitting the domain if necessary, specifying boundary constraints, and generating a mesh are all part of it. Next stage is solver setup. The solver setup is defined at this stage. Selecting the suitable CFD solver, choosing fluid characteristics, turbulence models, and other physical settings are all part of this process. Define the solver control parameters, such as convergence criteria and time steps, as part of the solver setup. The actual solution procedure begins after the pre-processing and solver setup are completed. It entails numerically calculating the governing equations of fluid flow over a particular domain and time step. The iterative solution procedure is repeated until the desired convergence requirements are reached. Following the completion of the solution process, in post-processing, the generated results must be visualized and analyzed. Visualizing flow fields, generating contour plots, streamlines, and vector plots, and extracting quantitative data such as pressure drop, flow rates, or forces acting on specific objects are all examples of post-processing operations. Lastly, validation stage. In this stage, the correctness and reliability of the CFD simulation results are evaluated by comparing them to experimental or analytical data. It contributes to the reliability and trustworthiness of the simulation results.

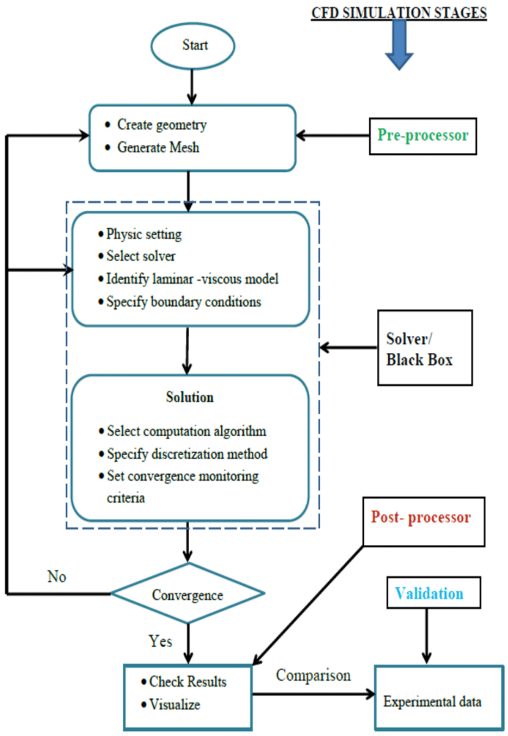

Figure 1 : Flowchart of CFD simulation

The following assumptions are made in order to examine the flow distribution across the parallel microchannels :

i. The fluid flow is steady, single phase, laminar, incompressible and three dimensional.
ii. Properties of and fluid are independent of temperature and pressure.
iii. Radiative heat transfer and surface roughness effects are negligible

The physical phenomena of fluid motion can be generally characterised in fundamental mathematical equations, usually in partial differential form, that regulate a process of interest and are frequently referred to as governing equations in CFD. The single phase model equations contain the continuity equation, momentum equation, and energy equation. The velocity vector is calculated using the continuity and momentum equations. Temperature distribution and wall heat transfer coefficient are calculated using the energy equation.

2.1 Model Description

There are four main stages in CFD analysis which are pre-processing, processing, post processing and validation. During pre-processing, Ansys Fluent will be used to create a three-dimensional model of a parallel microchannel heat sink. The computational setup for the parallel microchannel heat sink is as in Figure 2.

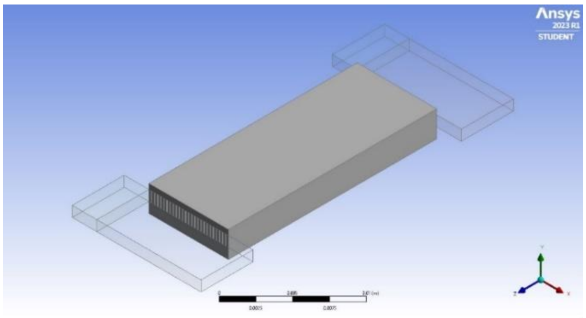

(a)

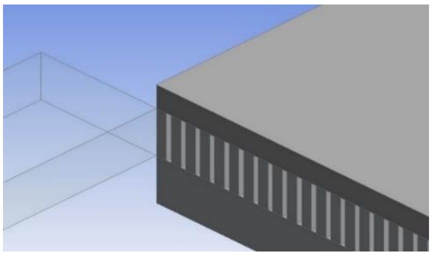

(b)

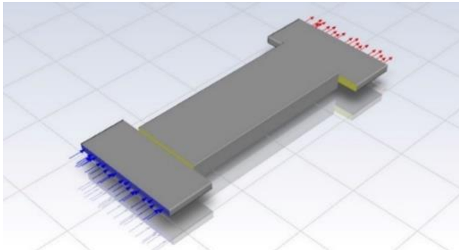

(c)

Figure 2 : Computational Setup of the Parallel Microchannel

These computational setup is design based on Sahar et al. (2023). The working fluid enters the intake manifold horizontally and exits the outlet manifold horizontally. The entrance manifold distributes the fluid to each microchannel, while the output manifold collects it. In this project, the inlet and output manifolds are 0.003366 m and 0.005 m in length and breadth, respectively. The depth of the manifolds is the same as the depth of the microchannel in this instance, 0.001 m.

2.2 Equations

The general form of continuity or mass, momentum and energy conservation equation used in ANSYS Fluent is shown in equation (1), (2) and (3) respectively.

Continuity :

$$\frac{\partial \rho}{\partial t} + \nabla * \left(\rho \vec{V}\right) = S_h \qquad (1)$$

This equation applies to both incompressible and compressible fluids. The mass transferred to the continuous phase from the dispersed second phase (e.g., vaporisation of liquid droplets) and other user-defined sources is represented by the source S_h. S_h is equivalent to zero in this study.

Momentum :

$$\frac{\partial \rho}{\partial t}(\rho\vec{V}) + \nabla * (\rho\vec{V}\vec{V}) = -\nabla p + \nabla * \left(\mu(\nabla\vec{V} + \nabla\vec{V}^T)\right) + \rho\vec{g} + \vec{F} \tag{2}$$

where ρ is the static pressure, $\rho\vec{g}$ is the gravitational body force and $\vec{F}$ is the external body force (e.g., caused by interaction with the dispersed phase). Other model-dependent source terms in $\vec{F}$ include porousmedia and user-defined sources.

Energy :

$$\frac{\partial}{\partial t}(\rho E) + \nabla * \left(\vec{V}(\rho E + P)\right) = \nabla * \left(k_{eff}\nabla T\right) + S_h \tag{3}$$

where k_{eff} is the effective conductivity ($k + k_t$), and k_t is the turbulent thermal conductivity (specified by the turbulence model employed). S_h contains the heat of chemical reaction as well as any other volumetric heat sources you've specified.

The equations (1) – (3) are solved using Ansys-Fluent software. The scale used in the meshing are in millimetres (mm). The flow in this study can be assumed laminar. Materials used in this study for fluid are air and water-liquid while for solid is aluminium. For solving the pressure-velocity coupling, Semi-Implicit Method for Pressure Linked Equations (SIMPLE) scheme was used. Gradient is discretized by least squares cell based, pressure is discretized by second order and for momentum and energy, both are discretized by first order upwind scheme. For boundary conditions, velocity-inlet is employed at the inlet, pressure-outlet is employed at the outlet and heat flux is prescribed at the base of the heat sink for all cases. A no slip boundary condition was assigned for all wall boundaries. The heat loss through the top cover was considered to be negligible. In this study, three different parameters were observed which are velocity, temperature and pressure. Six different of values for each velocity, temperature and pressure were used in this study to observe the distributions for each parameter across the channel.

2.3 Grid Validations

The hexa meshing grid scheme constructed in Ansys ICEM 14.5 was used to mesh the system. The quality of the generated mesh elements determines how accurate the CFD simulation results are. However, due to the limitation of number of grids, in this work only less than 512k nodes can be used. In this project, three different grid sizes were used to investigate the effect of grid sensitivity as shown in Figure 3. Based on Figure 3, it is observed that grid number 3 is the most suitable grid to use in this project as the calculation shown in the graph is converged.

Grid 1	2578 nodes 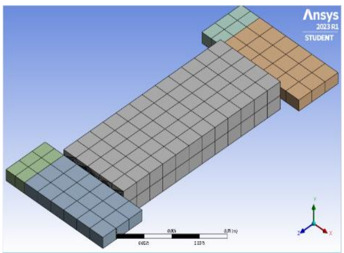 (a)	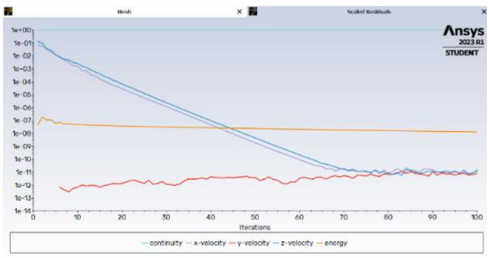 (b)

Grid 2	28134 nodes 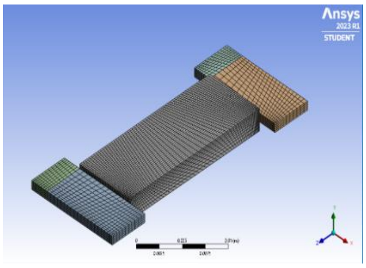 (c)	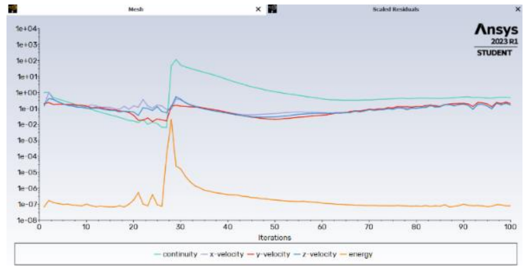 (d)
Grid 3	425586 nodes 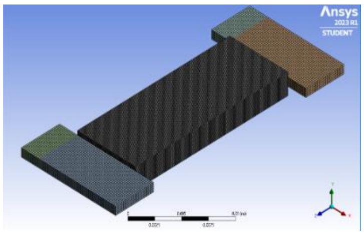 (e)	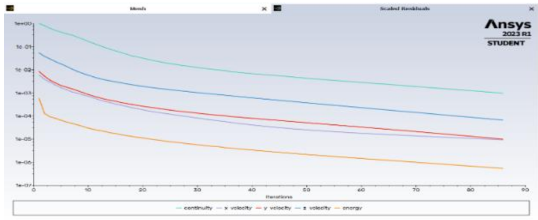 (f)

Figure 3 : Grid validation

3. Results and Discussion

The velocity contour and velocity profile for each value of velocity are shown in Figure 4. Based on the figures 4, it shows that the flow distribution across the channel is not uniformly distributed as the velocity-inlet increases. For example, at the higher inlet velocity condition which is 20 m/s, the flow ratio at the inlet is much smaller compared to the flow ratio at inlet for 1 m/s. Similar results were obtained from Sahar, (2019) where increasing the velocity inlet will cause flow maldistribution.

While this was going on, it was also made very evident that the channels at the lateral edges had a lower flow ratio than the channels at the centre. This is caused by losses that happen at the inlet manifold's sharp corners, as mentioned above, and illustrated in Figure 4. It implies that, the secondary flow caused by recirculating flow in the inlet manifold becomes more evident, as seen in Figure 4. In addition, Kumaraguruparan et al. (2011) concluded that flow separation or recirculation that took place at the inlet header or manifold was the cause of the flow maldistribution between channels. According to Wang et al. (2011), small flow separation zones were seen at the inlet manifold's sharp corners because of vortex flow, which decreased the flow rate in the channels.

In a microchannel, many kinds of variables affect the velocity in the channel's middle. The velocity profile, or how the fluid velocities are dispersed across the channel cross-section, is one crucial element. The velocity profile in laminar flow conditions is typically parabolic, with the highest velocity occurring at the microchannel's centerline and progressively declining towards the channel sides. As a result, the velocity along the centerline of the microchannel is typically higher than the velocity close to the walls. Same result was also obtained by Sahar, (2019) when compared to channels in the center, the flow ratio for the first and last channels is much lower at all inlet velocities. Furthermore, the distribution of velocity inside the microchannel is influenced by the velocity at the entrance. Generally speaking, larger intake velocities raise all microchannel velocities as well as those in the middle.

From the calculations of Reynold number, it is shown if the velocity at the inlet is increased, it will result in a higher Reynolds number. The Reynolds number is directly proportional to the velocity of the fluid. When the velocity is increased, the inertial forces within the flow become more dominant relative to the viscous forces. Greater Reynolds numbers result in a reduced friction factor, which increases non-uniformity.

The velocities used in this calculation is the average velocity obtained across the channel.

$\rho=998.2$, $\mu=0.001003$

$$D_h=L=\frac{2ab}{a+b}=\frac{2(0.001)(0.000209)}{0.001+0.000209}=0.00034574$$

where a = height of the channel , b = length of the channel

By using the equation; $Re=\frac{\rho VL}{\mu}$

a) Velocity: 1m/s
$$Re=\frac{(998.2)(0.0357016)(0.00034574)}{0.001003}=12.28$$

b) Velocity: 5m/s
$$Re=\frac{(998.2)(0.26588864)(0.00034574)}{0.001003}=91.49$$

c) Velocity: 10m/s
$$Re=\frac{(998.2)(1.096841071)(0.00034574)}{0.001003}=377.41$$

d) Velocity: 15m/s
$$Re=\frac{(998.2)(2.485709988)(0.00034574)}{0.001003}=855.30$$

e) Velocity: 20m/s
$$Re=\frac{(998.2)(3.628985393)(0.00034574)}{0.001003}=1248.68$$

f) Velocity: 25m/s
$$Re=\frac{(998.2)(4.48220581)(0.00034574)}{0.001003}=1542.26$$

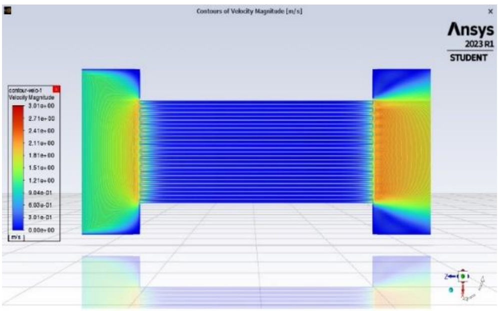
Ansys
2023 R1
STUDENT

(a)

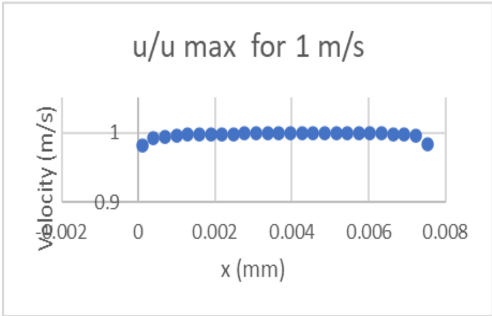
u/u max for 1 m/s
Velocity (m/s)
1
0.9
-0.002
0
0.002
0.004
0.006
0.008
x (mm)

(b)

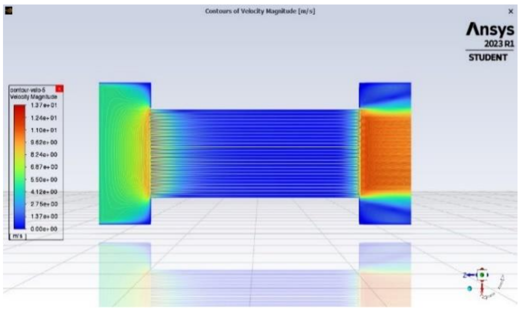
Ansys
2023 R1
STUDENT

(c)

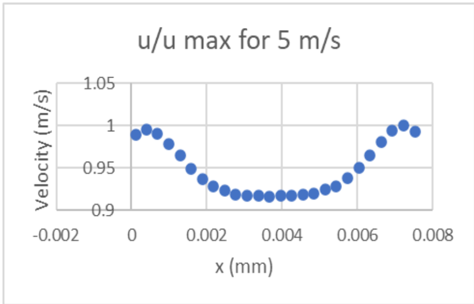
u/u max for 5 m/s
Velocity (m/s)
1.05
1
0.95
0.9
-0.002
0
0.002
0.004
0.006
0.008
x (mm)

(d)

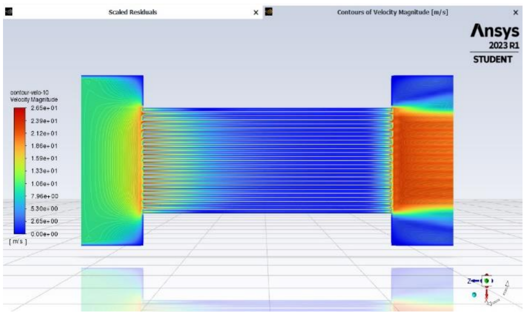
Ansys
2023 R1
STUDENT

(e)

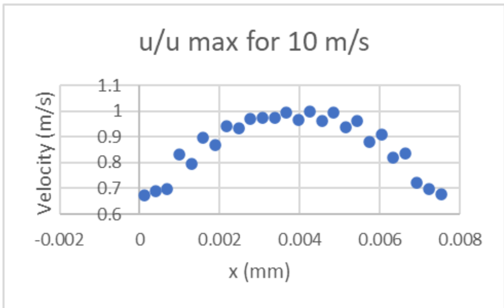
u/u max for 10 m/s
Velocity (m/s)
1.1
1
0.9
0.8
0.7
0.6
-0.002
0
0.002
0.004
0.006
0.008
x (mm)

(f)

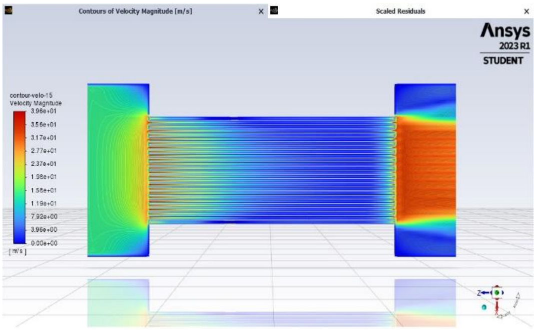

(g)

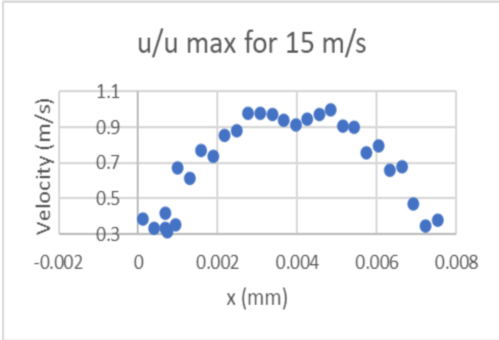

(h)

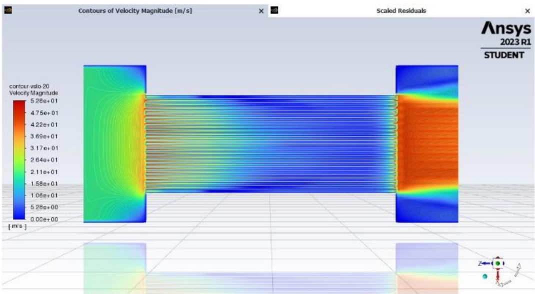

(i)

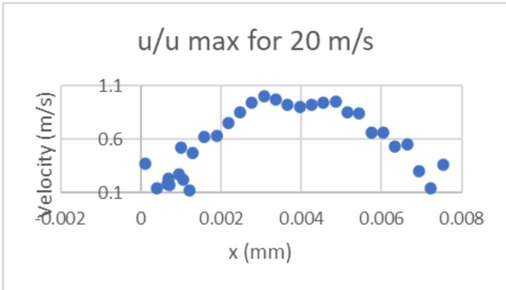

(j)

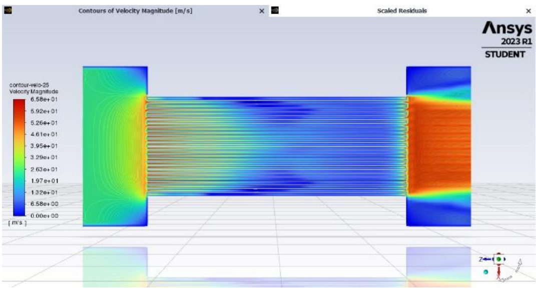

(k)

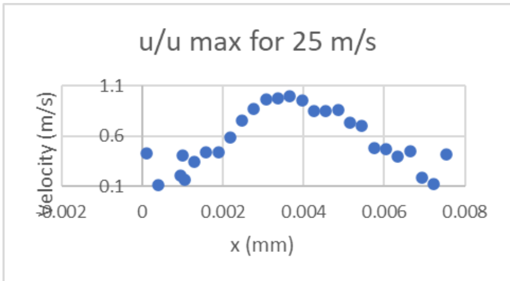

(l)

Figure 4 : Velocity Contour and Velocity Profile

For both Figure 5 and 6, only higher velocity inlet is chosen to see the temperature and pressure distribution across the channel. It is because as we can see from

Figure 4, it shows that the flow in the channel for velocity inlet 15 m/s, 20 m/ s and 25 m/s are nearing the middle of the channel.

Based on Figure 5, it can be seen that velocity-inlet does not give an impact on the temperature distribution as the temperature profile for all the velocity is slightly the same. The temperature remains uniformly distributed for all the velocity-inlet values. It is because velocity changes have an impact on flow distributions and convective heat transfer, they can also have an indirect impact on the temperature distribution. For instance, higher velocities can improve mixing and heat transfer rates, resulting in a more even distribution of temperature over the fluid domain. This was also observed by Xu et al. (2022) where as inlet air velocity increases from 2 m/s to 5 m/s, the maximum temperature of battery pack decreases in the range of 319.9–310.4 K, 325.1–313.9 K, 320.9–312.4 K, 327.9–318.9 K and 339.8–321.3 K at inlet position of 10 mm, 20 mm, 30 mm, 40 mm and 50 mm, respectively.

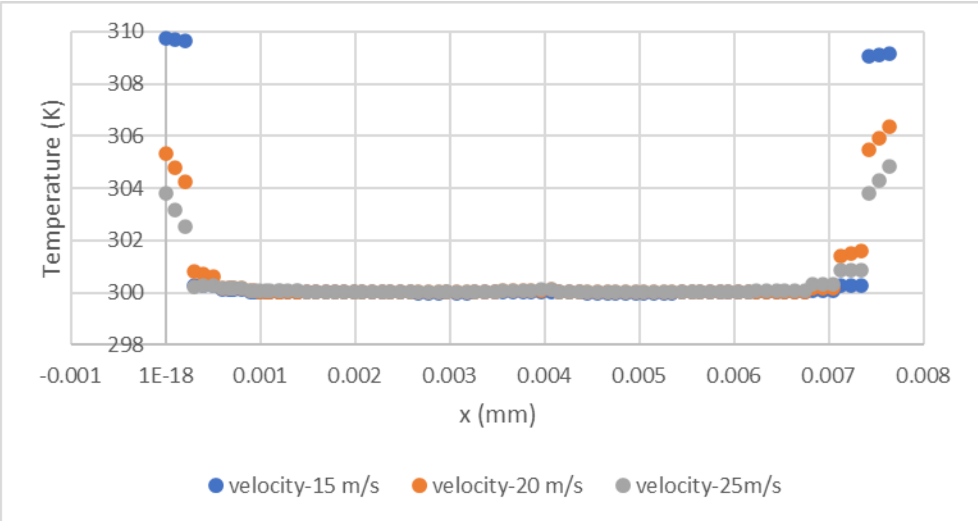

Figure 5 : Temperature distribution at different velocity inlet

From Figure 6, it shows that when the velocity is increasing, the pressure value also increases but it still shows a uniform flow distribution. This is due to the fluid flow's pressure distribution and input velocity are closely related concepts. Through Bernoulli's equation, which stipulates those changes in velocity are accompanied by commensurate changes in pressure, the velocity and pressure are connected. Variations in flow momentum and kinetic energy brought on by different inlet velocities might result in pressure fluctuations throughout the system. As a result, the velocity at the entrance may have an impact on the pressure distribution. The same results were obtained by Dziubak et al. (2023) where as the inlet velocity increases, the pressure values at the steering wheel face part are higher and higher.

It can be summarized that the velocity at the inlet can impact flow distribution, which, in turn, affect temperature and pressure distributions. The inlet velocity profile determines how the fluid is distributed within the channels and the overall flow characteristics. Changes in the velocity at the inlet can alter these flow patterns and subsequently influence the temperature and pressure distributions within the flow domain.

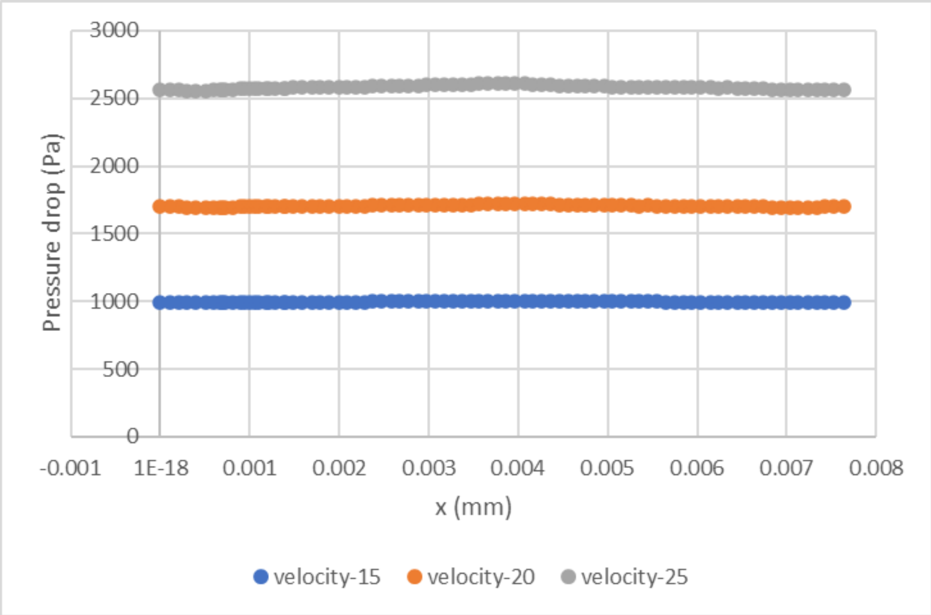

Figure 6 : Pressure distribution at different velocity inlet

Based on Figure 7, six different values of heat flux are used to see its effect on temperature distribution. It shows that the flow distribution for temperature is similar to each heat flux value. It was worth saying that the effect of different heat flux on temperature distribution was insignificant. It also shows that the temperature was uniformly distributed across the channel. It demonstrates that the heat flux is very high at the entrance of the microchannel as due to the thin thermal boundary layer then it decreases across the channel. The high heat flux in the entry region was also found by Sahar et al. (2016).

As the material used in this study is aluminum and it has high thermal conductivity which is $237\ Wm^{-1}K^{-1}$. Due to aluminum's high thermal conductivity, the impact of various heat fluxes on the temperature distribution in an aluminum solid is comparatively small. The extraordinary efficiency with which aluminum conducts heat is well recognised. An aluminum solid's strong thermal conductivity allows for the quick and even distribution of heat throughout the material when various heat fluxes are applied to it. As a result, temperature differences inside the solid are reduced, resulting in a generally uniform distribution of temperature. Aluminum's effective heat conduction makes it possible to minimise the effect of changing heat fluxes on temperature.

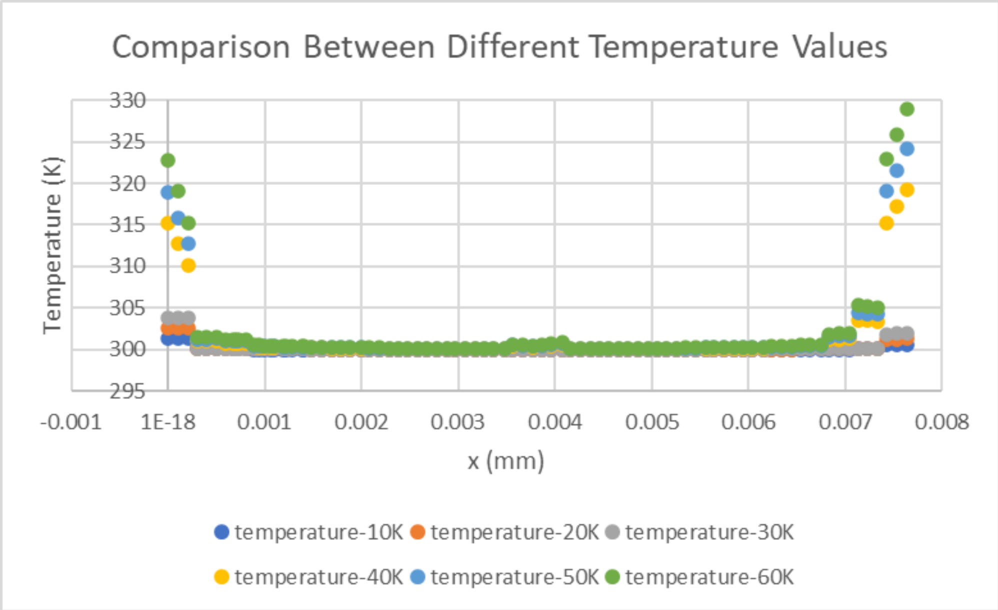

Figure 7 : Comparison between different temperature values

Figure 8 shows the pressure distribution across the channel for six different values of pressure. It can be seen that the pressure profile is the same for all values and higher pressure drives greater flow distribution. This relationship is known as Darcy's Law, which states that the pressure drop across a pipe is directly proportional to the fluid velocity and the length of the pipe. Therefore, the relationship between pressure drops and flow rate is proportional, and any change in one variable will affect the other. A study by Zhang et al. (2023) found that more gas flows into the channels in the centre area due to the inlet and outflow manifold's centre region's biggest pressure drop.

Because of the governing equations and assumptions of fluid mechanics, notably the incompressible flow assumption, the pressure profile is the same for all levels of the pressure. According to the incompressible flow assumption, regardless of changes in pressure, the fluid's density will not change. This presumption is frequently true for liquid flows or slow gas flows, when there are little density changes. This uniform pressure profile results from the instantaneous transmission of any pressure change throughout the fluid, which ensures that the pressure gradient is distributed uniformly throughout the flow domain. Since the driving forces and the flow resistance within the system are balanced, the pressure profile does not change with changes in pressure values. Instead, it represents this equilibrium. This phenomenon was also seen by Lee and Karayiannis (2023) where it is unlikely that the variation in pressure drop with system pressure has anything to do with how the flow distribution developed in the channels.

The Navier-Stokes equations and the continuity equation, which describe fluid flow, can be made simpler under the incompressible flow assumption. The mass flow rate entering and leaving a control volume must be equal, according to the continuity equation. The conservation of momentum is explained by the Navier-Stokes equations, which also link pressure gradients to fluid acceleration and viscous forces. This calculation has been proved by Maia et al. (2022).

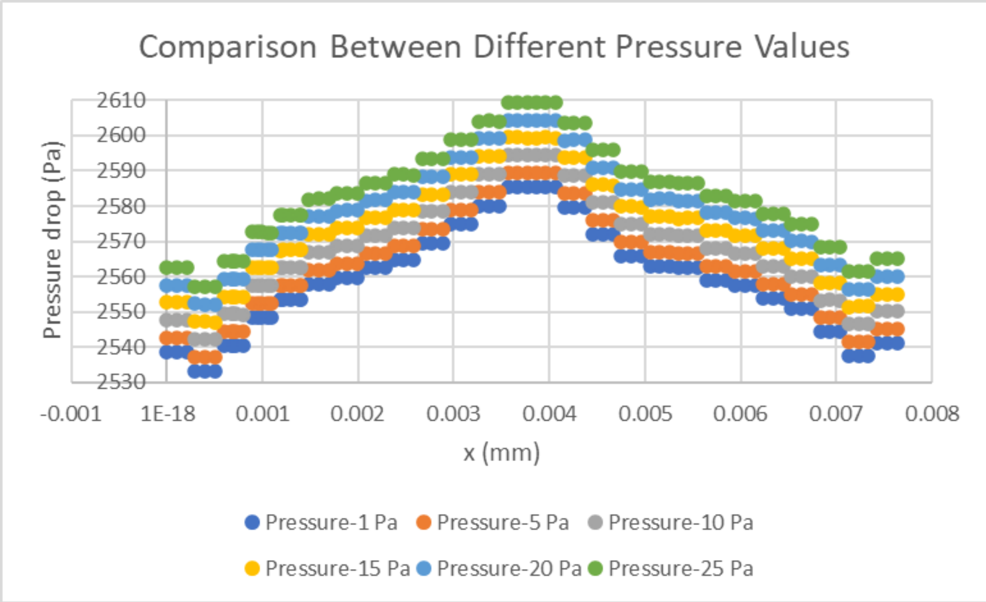

Figure 8 : Comparison between different pressure values

4. Conclusion

A numerical study of fluid flow and heat transfer in single phase in multi-microchannels was conducted using the computational software package, Ansys Fluent. The geometry construction and mesh generation were also performed in Ansys Fluent and the hexa mashing grid scheme was used for meshing. Rectangular multi-microchannel and water-liquid were used in this study. The effect of different values for velocity, pressure temperature towards the flow distribution was discussed in this study.

For velocity, as the velocity inlet increase, the distribution of the flow is not uniformly distributed. It also shows that the flow ratio around the edges of the channel is lower than the center due to the loses at the sharp edge. Next, for temperature, as the heat flux values increase, the temperature does not change drastically. It shows uniformly distributed flow across the channel. The velocity-inlet also does not affect the uniformly flow distribution. For pressure, as the value for pressure-outlet increase, the value for the pressure drops also increase and the pressure profile for all values are identically the same. When the velocity-inlet is varied, the pressure distribution remains uniformly distributed but the pressure value increase as the velocity increase.

The results of this study have substantial implications for the design and improvement of advanced cooling systems in numerous industries, including automotive applications, energy systems, and electronics cooling. Based on the results of the present thesis, there are still many open questions and discussions on fluid flow and heat transfer in single flow in multi-microchannel. The followings are the most important ones which could be considered and addressed in future studies such as further investigation of channel geometries, experimental validation and optimization techniques.

5. Acknowledgement

The authors grateful to Allah S.W.T for giving the strength to complete this project successfully. A sincere gratitude to everyone who volunteered their time and took part in the study for this project.

6. Funding

The author(s) received no specific funding for this work.

7. Conflict of Interest

The authors have no conflicts of interest to declare.

8. References

Dziubak, T., Dziubak, S., & Tomaszewski, M., (2023). Numerical study of the effect of axial cyclone inlet velocity and geometrical parameters on separation efficiency and pressure drop. *Powder Technology*, *427*(March). https://doi.org/10.1016/j.powtec.2023.118692

Kumaraguruparan, G., Kumaran, R. M., Sornakumar, T. & Sundararajan, T., (2011). A numerical and experimental investigation of flow maldistribution in a micro-channel heat sink. *International Communication in Heat and Mass Transfer*, Volume 38, pp. 1349-1353. https://doi.org/10.1016/j.icheatmasstransfer.2011.08.020

Lee, V. Y., & Karayiannis, T. G., (2023). Influence of system pressure on flow boiling in microchannels. *International Journal of Heat and Mass Transfer*, *215*, 124470. https://doi.org/10.1016/j.ijheatmasstransfer.2023.124470

Maia, A. A. G., Cavalca, D. F., Tomita, J. T., Costa, F. P., & Bringhenti, C. (2022). Evaluation of an effective and robust implicit time-integration numerical scheme for Navier- Stokes equations in a CFD solver for compressible flows. *Applied Mathematics and Computation*, *413*, 126612. https://doi.org/10.1016/j.amc.2021.126612

Pan, M., Tang, Y., Pan, L. & Lu, L., (2008). Optimal design of complex manifold geometries for uniform flow distribution between microchannels. *Chemical Engineering Journal*, Volume 137, pp. 339-346. https://doi.org/10.1016/j.cej.2007.05.012

Qin, H., Li, X., Zhang, L., & Wu, X., (2023). Flow distribution in the air cooler of HTGR passive cavity cooling system. *Annals of Nuclear Energy*, *180*(July 2022), 109478. https://doi.org/10.1016/j.anucene.2022.109478

Qu, W., Mudawar, I., Lee, S.-Y. & Wereley, S., (2006). Experimental and computational investigation of flow development and pressure drop in rectangular micro-channel. *Journal of Electronic Packaging* , Volume 128, pp. 1-9. https://doi.org/10.1115/1.2159002

Sahar, A. M. (2019). *Computational Fluid Dynamics of Single and Two Phase Flow in Microchannels*. College of Engineering, Design and Physical Sciences Brunel University London.

Sahar, A. M., Ishak, M. S. A., Wissink, J., Mahmoud, M. M., & Karayiannis, T. G., (2023). Flow distribution in parallel rectangular multi microchannels in single phase. *CFD Letters*, *15*(1), 67–75. https://doi.org/10.37934/cfdl.15.1.6775

Sahar, A. M., Ozdemir, M.R., Fayyadh, E.M., Wissink, J., Mahmoud M. M. and Karayiannis, T. G., (2016). Single phase flow pressure drop and heat transfer in rectangular metallic microchannels. *Applied Thermal Engineering*. 93:1324-1336. https://doi.org/10.1016/j.applthermaleng.2015.08.087

Tuckerman D. B. and Pease R. F. W., (1981) High-performance heat sinking for VLSI. *IEEE Electron Device Letters*, vol. 2, no. 5, pp. 126-129. https://ieeexplore.ieee.org/document/1481851

Wang, C.-C., Yang, K.-S., Tsai, J.-S. & Chen, I. Y., (2011). Characteristics of flow distribution in compact parallel flow heat exchangers, part I: Typical inlet header. *Applied Thermal Engineering*, Volume 31, pp. 3226-3234. https://doi.org/10.1016/j.applthermaleng.2011.06.004

Xu, Z., Yu, G., Zhang, T., & Wang, R., (2022). Cooling performance of battery pack as affected by inlet position and inlet air velocity in electric vehicle. *Case Studies in Thermal Engineering*, 39, 102382. https://doi.org/10.1016/j.csite.2022.102382

Zhang, W., Zeng, Y., Zhang, H., Shi, R., Duan, N., Jia, L., Yan, D., (2023). Structural design and optimization for a 20-cell solid oxide fuel cell stack based on flow uniformity and pressure drop. *International Journal of Hydrogen Energy*, 0360-3199, https://doi.org/10.1016/j.ijhydene.2023.05.325